Item 838-H-15
NAS 1.60:1670
COMPLETED
MAY 2

NASA Technical Paper 1670

ORIGINAL

Multistage Depressed Collector With Efficiency of 90 to 94 Percent for Operation of a Dual-Mode Traveling-Wave Tube in the Linear Region

Peter Ramins and Thomas A. Fox

APRIL 1980

NASA

16

NASA Technical Paper 1670

Multistage Depressed Collector With Efficiency of 90 to 94 Percent for Operation of a Dual-Mode Traveling-Wave Tube in the Linear Region

Peter Ramins and Thomas A. Fox
Lewis Research Center
Cleveland, Ohio

National Aeronautics
and Space Administration

**Scientific and Technical
Information Office**

1980

Summary

An axisymmetric multistage depressed collector of fixed geometric design was evaluated in conjunction with an octave-bandwidth, dual-mode traveling-wave tube (TWT). The TWT was operated over a wide range of conditions to simulate different applications. The collector performance was optimized (within the constraint of fixed geometric design) over the range of TWT operating conditions covered.

For operation of the TWT in the linear, low-distortion range, 90 percent and greater collector efficiencies were obtained, leading to TWT overall efficiencies of 20 to 35 percent, as compared with 2 to 5 percent with an undepressed collector. With collectors of this efficiency and minimized beam interception losses, it becomes practical to design dual-mode TWT's such that the low mode can represent operation well below saturation. Consequently, the required pulse-up in beam current can be reduced or eliminated and this mitigates beam control and dual-mode TWT circuit design problems.

For operation of the dual-mode TWT at saturation, average collector efficiencies in excess of 85 percent were obtained for both the low and high modes across an octave bandwidth, leading to a three- to four-fold increase in the TWT overall efficiency.

Introduction

In a joint USAF-NASA program, the Lewis Research Center is conducting an efficiency improvement program on traveling wave tubes (TWT's) for use in electronic countermeasure (ECM) and communication systems by applying the multistage-depressed-collector (MDC) and spent-beam-refocusing techniques developed at Lewis (refs. 1 to 4). These techniques convert part of the kinetic power of the spent electron beam at the TWT output to useful electric power. Therefore, the prime power required to operate the tube can be substantially reduced, and the heat dissipation problem mitigated.

The detailed characteristics of the spent electron beam can vary widely, both with the individual TWT design and with the operating point within the range dictated by the individual TWT application. Consequently, optimum refocusing-system and MDC designs must function effectively over the entire range of required TWT operating points and must be produced on an individual basis for each specific application of each TWT.

An octave-bandwidth, periodic-permanent-magnet (PPM) focused, dual-mode TWT (Teledyne MEC MTZ 7000, serial number 103) was operated over a wide range of conditions to simulate the application where

(1) The TWT must be operated at constant output power in the linear, low-distortion range (typically 4 dB or more below saturation) and consequently at very low electronic efficiencies (e.g., 2 to 4 percent for the application discussed in ref. 5)

(2) A large (10:1) pulse-up capability in the output power is needed, and the low-mode represents TWT operation well below saturation

(3) The electron beam in the TWT must be "on" at all times, but the TWT is in a standby mode (no rf input) most of the time

(4) An octave bandwidth, dual-mode TWT is pulsed (at saturation) between the low and high modes.

The axisymmetric MDC (shown in fig. 1) and a refocusing system were added to the TWT, and collector performance was individually optimized (within the constraint of fixed collector geometric design) for each of the above applications. The results of these tests are reported hereinafter.

The results of a similar test program with Teledyne MEC MTZ 7000, serial number 102, are reported in reference 6. This TWT, however, exhibited excessive circuit and beam-interception losses, which severely limited the overall TWT efficiencies attainable. Serial number 103 is believed to be a more typical example of this class of TWT's.

Symbols[1]

B_z	axial magnetic field, T
e	electronic charge
I_B	true interception current in forward direction
I_{body}	$I_B + I_S$
I_{En}	collector current to n^{th} electrode
I_{E1}	backstreaming current to undepressed collector electrode

[1]See also figs. 2 and 3.

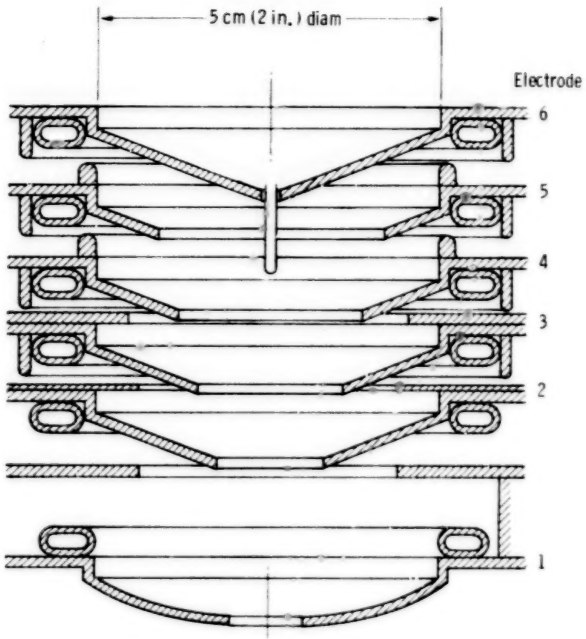

Figure 1. - Multistage depressed collector (MDC).

I_k cathode current or beam current

I_S backstreaming current to TWT body

P_{body} (total rf losses in TWT) + (true beam interception losses)

P'_{body} P_{body} + (all or part of backstreaming power)

P_{coll} total power in spent beam that enters MDC

P_{fund} radiofrequency output associated with fundamental frequency

P_{hrm} radiofrequency output resulting from haromonic frequencies

P_{rf} total rf output ($P_{fund} + P_{hrm}$)

P_{therm} $P_{rf} + P'_{body}$ + (total collector dissipation)

P_{tot} prime power, ($V_k I_k - P_{recovered}$)

(r,θ,z) cylindrical coordinates

$\overline{V}$ average potential of intercepted elecrons

V_k cathode potential (always negative for work reported herein)

Experimental TWT and MDC Performance Evaluation

To obtain complete and accurate TWT and MDC performance evaluations, it is necessary to determine the final power distribution in the system. This distribution is shown in figure 2 in the form of

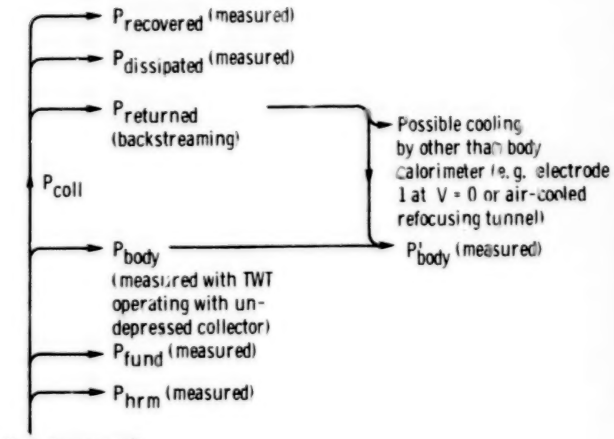
$P_{recovered}$ (measured)
$P_{dissipated}$ (measured)
$P_{returned}$ (backstreaming)
Possible cooling by other than body calorimeter (e.g. electrode 1 at V = 0 or air-cooled refocusing tunnel)
P_{coll}
P_{body} (measured with TWT operating with un-depressed collector)
P'_{body} (measured)
P_{fund} (measured)
P_{hrm} (measured)
V_k I_k (measured)
P_{body} = (rf circuit losses) + (intercepted power in forward direction)
P'_{body} = P_{body} + (all or part of backstreaming power)
$P_{coll} = V_k I_k - P_{rf} - P_{body}$
Collector efficiency = $P_{recovered}/P_{coll}$

(a) Power flow.

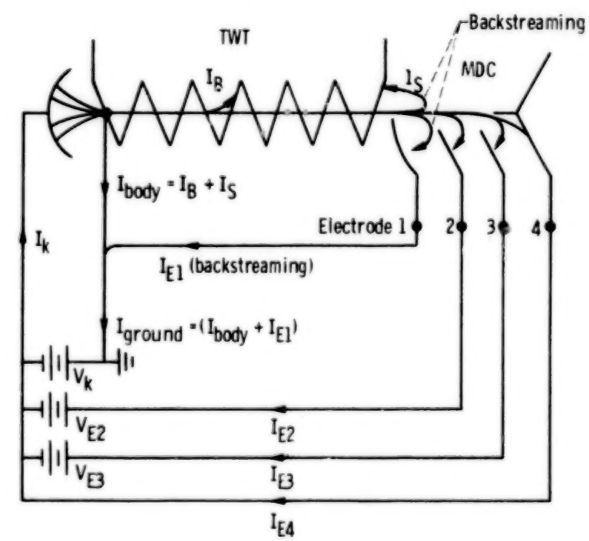

Prime power = $V_k(I_{ground}) + \sum_{n=2}^{4} V_{En} I_{En}$

$P_{recovered} = \sum_{n=2}^{4} \left(|V_k - V_{En}|\right)(I_{En})$

$P_{coll} = V_k I_k - P_{rf}$ - (circuit losses) - $(I_B \overline{V})$ where $e\overline{V}$ is average energy of intercepted electrons

$P_{coll} \neq V_k I_k - P_{rf}$ - (circuit losses) - $(I_{ground} V_k)$

(b) Electron flow.

Figure 2. - Flow diagrams for TWT with MDC.

power-flow and electron-flow diagrams for a TWT with a depressed collector. Part of the initial beam power ($I_k V_k$) appears as measured radiofrequency (rf) output power at the fundamental and (possibly) harmonic frequencies, and part is dissipated by the TWT body as the sum of rf losses in the TWT and intercepted beam power in the forward direction. The rest of the beam power enters the collector. Part of this kinetic power is recovered as useful electric power, and part is dissipated as thermal power on the collector plates. Collector efficiency is defined as

$$\frac{P_{recovered}}{P_{coll}}$$

With a depressed collector, the possibility exists of backstreaming electrons (I_S and I_{E1} in fig. 2(b)) returning significant power to the TWT body. Since any backstreaming produced by the depressed collector must be accounted for in determining efficiency, this backstreaming power must be evaluated and charged against the depressed collector, or exaggerated collector efficiencies will result. A more complete discussion of this problem can be found in reference 7.

It should be noted that neither P_{coll}, P_{body}, nor true beam interception I_B can be measured directly for a tube operated with an MDC. Without these measured values, the determination of MDC efficiencies requires certain assumptions that can significantly affect the computed collector performance:

(1) Assumption of the circuit losses (rf losses on the rf structure)

(2) Assumption of the true intercepted current in the forward direction

(3) Assumption of the average energy of the intercepted electrons.

With these assumptions P_{coll} can be computed from the equation

$$P_{coll} = V_k I_k - (\text{circuit losses}) - (I_B \overline{V}) - P_{rf}$$

as shown in figure 2(b).

However, it has been our experience at Lewis that both the circuit losses and the true beam interception can vary widely, even between TWT's of identical design (ref. 8). Circuit losses at a given frequency can be strongly affected by reflections due to mismatches (individual TWT imperfections), and the TWT's are usually focused to meet system specifications, not to produce minimum beam-current interception.

The need for making any assumptions can be avoided entirely only by first operating the same TWT with a suitable thermally isolated undepressed collector. The power returned to the TWT body by backstreaming electrons (secondaries) from such a collector is negligible. The power flow diagram for a

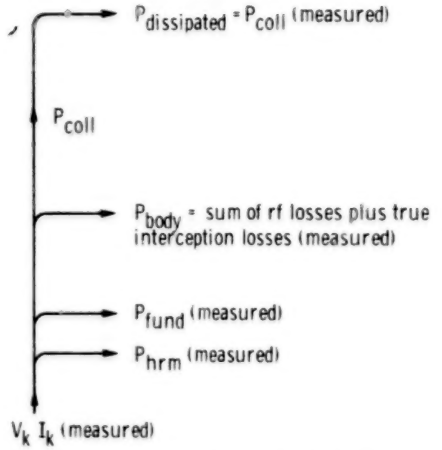

Figure 3. - Power flow diagram for TWT with undepressed collector.

TWT with an undepressed collector is shown in figure 3. The power into the collector P_{coll} can be measured directly, or alternatively, P_{rf} and P_{body} can be thermally measured and P_{coll} computed from measured quantities. Since only the total body power P_{body} is needed for the computation of P_{coll}, it can be seen that with this experimental approach the questions of circuit efficiency, true interception, and the average energy of the intercepted electrons are irrevelant.

Experimental TWT

The Teledyne MEC model MTZ 7000 (TWT 103) as modified for use in this program and its performance characteristics are shown in figure 4. A refocusing system consisting of two coils has been added, and the TWT is mounted on a 25.4-centimeter (10-in.) ultrahigh-vacuum (UHV) flange. The UHV valve shown was designed to keep the TWT under vacuum during MDC installation and changes, facilitating startup and minimizing cathode activation problems (ref. 9).

This TWT was delivered with an undepressed thermally isolated water-cooled collector mounted on a matching 25.4-centimeter (10-in.) vacuum flange. This special collector was required for the bench test.

Experimental Arrangement

Bench Test

The purpose of the bench test was to document the performance of the TWT as delivered with an undepressed spent-beam collector so that TWT performance changes, if any, due to the MDC can be determined and so that accurate MDC efficiency measurements could later be made. The rf load,

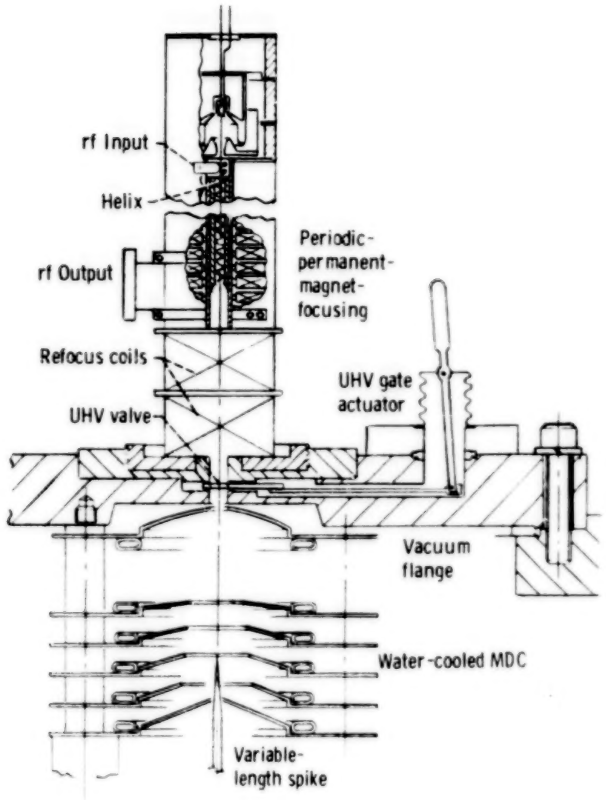

Figure 4. - Schematic of MEC TWT 103 with MDC. Frequency, 4.8 to 9.6 GHz; total maximum rf output, 510 W in low mode and 830 W in pulsed-up mode; cathode potential, 9930 V; beam current, 0.38 A in low mode and 0.49 A in pulsed-up mode; duty cycle, 100 percent in low mode and 20 percent in pulsed-up mode.

TWT body, and collector are all thermally isolated and water cooled. Thermal power to each is measured by a combination of flowmeter and thermopile. Since the collector is undepressed, the power returned to the TWT by any backstreaming electrons is negligible. The measured P_{body} is, therefore, the sum of the total rf losses in the TWT and the interception losses.

Multistage Depressed Collector Test

In the MDC test setup (fig. 5) the TWT is mounted on a matching flange on a UHV system. The MDC is mounted directly on the UHV flange, which houses the TWT and vacuum valve. Each MDC electrode, including the undepressed electrode, is thermally and electrically isolated and is water cooled. The spent-beam power recovered by each MDC electrode, as well as the thermal (kinetic) power dissipated on each electrode, was measured. A vacuum feedthrough drives a variable-length spike. Over its range of variability, the length of the spike significantly affects the electric-field distribution within the collector, and its optimum length can be established quickly and easily for each MDC configuration. Since the refocusing coils and pole pieces are outside the vacuum, they can be manipulated and moved over their designed range of variability while the TWT is operating. Together with variation of the refocusing coil currents, this enables the rapid optimization, within limits, of the refocusing field profile. Once established, this profile can be synthesized with a permanent-magnet refocusing system.

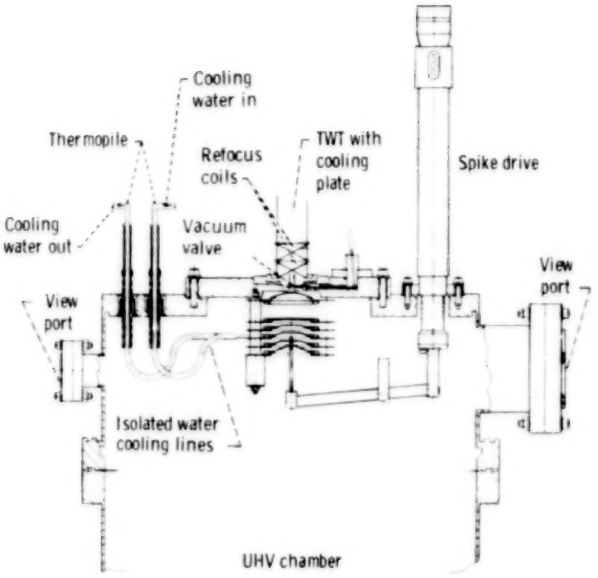

Figure 5. - Schematic of MDC measuring system.

A typical experimental collector arrangement is shown in figure 5. This fully demountable mechanical design was chosen for experimental convenience. Separate water cooling and calorimetry of each collector electrode were chosen for diagnostic purposes and for the system's ability to provide information for the eventual thermal design of a conduction-cooled MDC.

The internal active volume of the MDC is that within the inner diameter of the cooling lines (i.d., 5.1 cm). The electrode geometries within this volume are critical to the MDC performance, but the passive electrode support structure outside is not. Extensive thermal and mechanical design changes will have to be made to adapt these MDC's to practical TWT's.

A novel data acquisition system was used to optimize collector efficiency under various conditions. This system provides an analog real-time readout of the recovered power as any of the system variables are changed while the TWT is operating. These variables are the individual collector stage voltages,

the refocusing coil currents, the polepiece locations, and the spike length.

Maximizing recovered power is identical to maximizing the MDC efficiency. Once the optimum combination of operating conditions is found, an automated system is used for actual data taking.

Experimental Program and Results

Traveling-Wave Tube Bench Test

The dual-mode TWT with an undepressed collector was operated at saturation across the octave bandwidth in both the low and high modes. In addition, at selected operating frequencies the TWT performance and fixed TWT losses were evaluated at rf powers as much as 12 decibels below saturated output power. Bench test data in the low mode were obtained at a duty cycle of 20 percent (instead of continuous-wave (cw) operation) because of the limited heat handling capability of the undepressed spent-beam collector: in previous tests with identical undepressed spent-beam collectors (refs. 2 and 8), it was found that extreme heating of parts of the collector led to migration of copper to the output section of the TWT. Data in the high mode were obtained at a duty cycle of 10 percent.

The rf output power at the fundamental frequency, the TWT body losses (sum of rf losses and interception losses), and total, fixed TWT losses (sum of TWT body losses and harmonic power generated) as functions of frequency are shown in figures 6(a) and (b) for the low and high modes, respectively. The average beam interception at saturation was 1.1 and 1.9 percent for the low and high modes, respectively. Minimized beam interception is of particular significance for operation of the TWT in the linear region because the relative contribution of rf losses to the total fixed TWT losses decreases rapidly because of the combination of reduced electronic efficiency and reduced rf circuit heating.

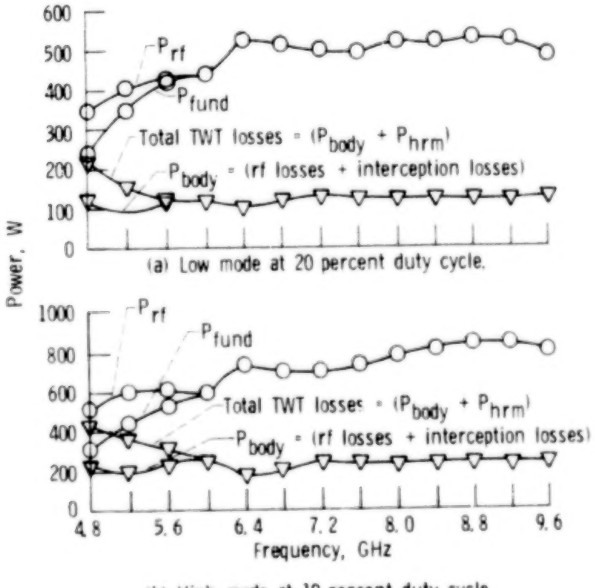

Figure 6. - Radiofrequency power and TWT losses versus frequency at saturation for TWT 103.

For both the low and high modes the rf output power at the fundamental frequency P_{fund} dropped off dramatically near the low band edge. Harmonic injection is normally used with production models of this TWT to boost P_{fund} at the low band edge. However, because it was impossible to duplicate the unknown system input drive conditions with laboratory components, all results obtained during this program were with input drive at only the fundamental frequency.

To calculate the circuit efficiency of the TWT, it is necessary to make an assumption about the average energy of the intercepted electrons. Figure 7 shows

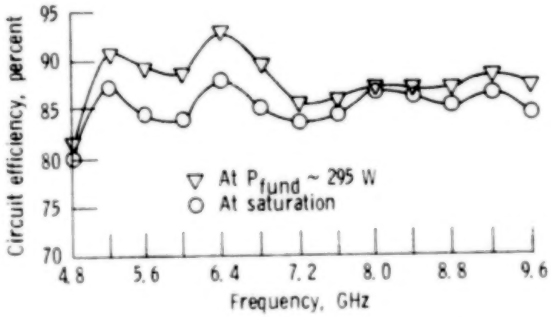

Figure 7. - Circuit efficiency versus frequency. Low mode of TWT 103 at a duty cycle of 20 percent.

the circuit efficiency of TWT 103, at saturation and at constant output power, in the low mode as a function of frequency for an average intercepted electron energy of (1 - electronic efficiency)eV_k. Where harmonic power is generated, the circuit efficiency is based on the total rf power generated, since it is impossible to separate the contributions to the total circuit losses due to P_{fund} and P_{hrm}. Attenuator and sever losses are included in the circuit losses because it is impossible to separate their contribution to the measured P_{body}. Based on computations made by H. G. Kosmahl of Lewis with the large-signal helical TWT computer program described in reference 10, the total sever and attenuator losses of this TWT are about 1½ percent of the total rf power generated.

Comparing the results at saturation and at P_{fund} = 295 watts reveals that additional circuit heating is taking place when operating at saturation, even at a duty cycle of 20 percent. A stronger effect might be expected for cw operation (ref. 8). The rf losses as a function of frequency do not exhibit the frequency dependence that would be expected from a combination of skin effect and dielectric losses. Losses due to mismatches can have very significant effects.

After completion of the bench test, the UHV valve (see fig. 4) was closed, and the undepressed spent-beam collector removed. The TWT was kept under a hard vacuum during the subsequent MDC installation and no processing (gradual outgassing) of the TWT was required.

Multistage Depressed Collector Test Results

The collector shown in figure 1 was added to the TWT, and the combination evaluated. The MDC was operated in three-, four-, and five-stage configurations. The number of MDC stages is defined as the number of distinct voltages (other than ground potential) needed to operate the MDC. In the three-stage configuration electrodes 2 and 3 and electrodes 4 and 5 were electrically connected (see fig. 1). In the four-stage configuration electrodes 2 and 3 were electrically connected. For all of the configurations, the most depressed stage (electrode 6 in fig. 1) was always operated at cathode potential.

The single MDC geometric design used in these tests had been experimentally optimized for a cw TWT (Teledyne MEC 5897C) operating at an electronic efficiency of 17 percent. Within this constraint of fixed geometry (not optimum for this dual mode TWT or for a broad range of operating conditions), the MDC performance was optimized for the various operating conditions discussed above by varying

(1) The electrode voltages

(2) The refocusing system profile

(3) The MDC spike length.

Data for the low and high modes were obtained at duty cycles of 100 and 20 percent, respectively. Collector efficiencies (see fig. 2(a)) were determined using the values of P_{body} as measured at duty cycles of 20 and 10 percent for the low and high modes, respectively. The effect of any additional circuit heating at the higher duty cycles used for MDC tests was not investigated in detail. Such heating, if any, would lead to underestimated collector efficiencies.

A coating of carbon black on electrodes 2 to 6 (see fig. 1) was used to suppress secondary-electron emission from the MDC collecting surfaces. The role of secondary electrons in this type of MDC is discussed in reference 2.

Final energy balance of the TWT-MDC system. – An example of the data obtained and the energy (power) balance established at a specific operating point is shown in table I. The currents, voltages, and powers have been rounded off after computation.

The total rf power generated, the TWT body losses, including any backstreaming to the TWT body, and the power dissipated in the MDC, including backstreaming to the undepressed electrode, are all thermally measured. Their sum is P_{therm}. The possibility exists, however, of some backstreaming electrons (part of I_s, but not measured separately) being collected in the air-cooled section of the refocusing tunnel. No attempt was made to measure the resulting thermal dissipation directly. Such backstreaming shows up as the difference between P_{tot} and P_{therm} (22 W for the example in table I). The consistency of the measurements (beyond the ½ percent power balance already established) can be checked by computing the average energy of the electrons backstreaming to the TWT and refocusing tunnel from:

$$\frac{E}{e} = \frac{(P'_{body} - P_{body}) + (P_{tot} - P_{therm})}{I_s}$$

For the case shown in table I, E = 6.4 keV/electron. This compares very closely to the average energy of 60 W/9.5 mA = 6.3 keV/electron computed for the backstreaming electrons collected on the undepressed electrode (collector electrode 1 in table I).

TWT-MDC performance for operation of the TWT in the linear range. – The TWT was operated over its linear range in the low mode to simulate applications where the TWT must be operated at constant output power in the linear, low-distortion range and consequently at very low electronic efficiencies (e.g., 2 to 4 percent for the application discussed in ref. 5). The MDC performance was individually optimized at each TWT operating point.

The results are shown in table II for the operating frequency (6.4 GHz) which produced minimum fixed TWT losses (see fig. 6). The collector and TWT overall efficiencies obtained with the three MDC's are compared in figures 8 and 9, respectively. Each collector produced, over the operating conditions covered, a very dramatic improvement in the overall efficiency: from a factor of 6 to 15 for the three-stage collector to a factor of 7 to 18 for the five-stage collector. The four- and five-stage collector efficiencies exceeded 90 percent over the entire range. Figures 8 and 9 show that the improvement obtained from additional stages (four versus three and five versus four) decreased for operation increasingly below saturation. For these collectors this is due to the fact that, at very low levels of electronic efficiency, most of the spent beam was collected on the upper stages (electrodes 4 and 5 in fig. 1) and the optimum (five

TABLE I. - RESULTS FOR TWT 103 WITH FIVE-STAGE COLLECTOR DEMONSTRATING FINAL ENERGY BALANCE AT A REPRESENTATIVE FREQUENCY

(a) Tube test conditions and results

Frequency, GHz	9.2
P_{in}, mW	180
P_{fund}, W	501
P_{hrm}, W	0
Gain, dB	34
Duty cycle, percent	100
V_k, kV	9.92
I_k, mA	381
Beam power, W	3780
P_{body}, W	121
P'_{body}, W	136
I_B, mA	4.4
I_S, mA	5.8

(b) MDC test conditions and results

Collector electrode	Voltage,[a] kV	Current, mA	Power, W	
			Recovered	Dissipated
1	0	9.5	0	60
2	-5.56	70.2	390	62
3	-6.10	93.0	568	91
4	-7.74	49.1	380	34
5	-9.45	146.8	1387	90
6	-9.92	1.9	19	40
Total			2744	376

Collector efficiency, 86.9 percent
Overall efficiency, 48.4 percent
P_{therm} = 1014
P_{tot} = 1036

(c) Final energy balance

Useful rf power, W	501
TWT body losses, W	121
Backstreaming to TWT body, W	15
Backstreaming to refocusing tunnel,[b] W	22
Backstreaming to undepressed collector, W	60
Collector (2 to 6) dissipation, W	317
Recovery power, W	2744
	Total 3780

[a]With respect to ground potential.
[b]Computed from (P_{tot} - P_{therm}).

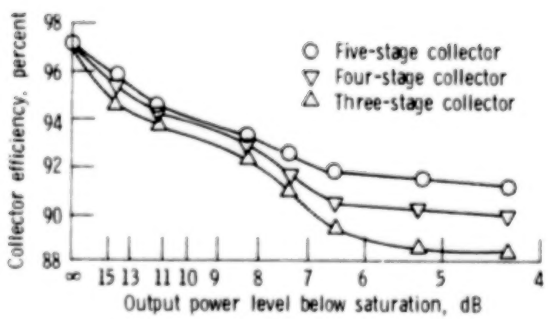

Figure 8. - Collector efficiency versus output power level below saturation. Linear range of low mode at 6.4 GHz.

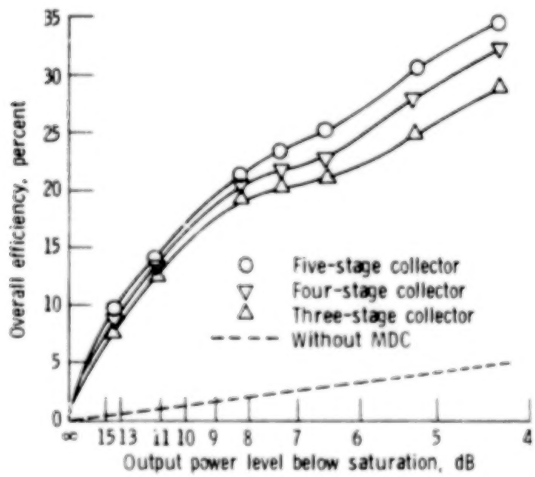

Figure 9. - Overall efficiency versus output power level below saturation. Linear range of low mode at 6.4 GHz.

stage) voltages of these electrodes differed by only a few hundred volts. Typical collector voltages (normalized to V_k) for operation of the TWT in the linear range were

(1) Five stage – 1.0, 0.98, 0.96, 0.72, and 0.58
(2) Four stage – 1.0, 0.97, 0.93, and 0.66
(3) Three stage – 1.0, 0.97, and 0.71.

Similar results were obtained when the optimizations were performed at other frequencies.

In order to evaluate the TWT-MDC performance as a function of frequency for a fixed set of MDC operating conditions, the TWT and four-stage collector were operated over an octave bandwidth at constant output power P_{rf}. The results are shown in figure 10(a). It is evident that the MDC performance is highly insensitive to the operating frequency as such.

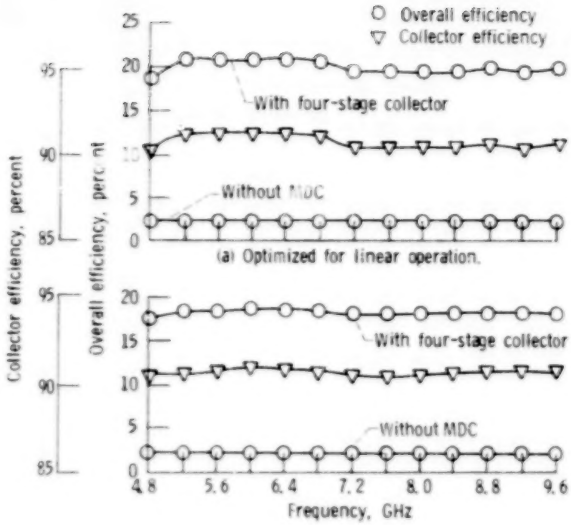

(b) Compromise optimization favoring 10:1 point of low mode.

Figure 10. – TWT overall and four-stage collector efficiencies versus frequency at constant total rf output power for a fixed set of MDC, and refocusing-system operating conditions.

TABLE II. – DUAL MODE TWT-MDC PERFORMANCE FOR OPERATION IN THE LINEAR RANGE (LOW MODE AT 6.4 GHz)

(a) Five-stage collector

Output power level below saturation dB	Overall efficiency, percent		Collector efficiency, percent
	Without MDC	With MDC	
4.3	5.0	34.6	91.2
5.3	4.0	30.6	91.5
6.6	3.0	25.2	91.8
7.4	2.5	23.4	92.6
8.3	2.0	21.3	93.3
11.4	1.0	14.0	94.7
14.1	.53	9.7	95.8
dc beam	----	----	97.2

(b) Four-stage collector

4.3	5.0	32.2	90.0
5.3	4.0	27.9	90.3
6.6	3.0	22.9	90.5
7.4	2.5	21.7	91.7
8.3	2.0	20.5	93.0
11.3	1.0	13.6	94.4
14.2	.51	8.8	95.4
dc beam	----	----	97.1

(c) Three-stage collector

4.3	5.0	28.9	88.4
5.3	4.0	24.8	88.6
6.5	3.0	21.0	89.4
7.4	2.5	20.3	91.0
8.3	2.0	19.2	92.3
11.2	1.0	12.6	93.8
14.2	.52	7.7	94.6
dc beam	----	----	97.1

Dual-mode TWT-MDC performance for a 10:1 pulse-up in output power. – For certain applications, both in ECM and communications (ref. 5), a large (up to 10:1) pulse-up capability in output power is required. The approach commonly used to achieve this is to pulse up the beam current. Typically, beam current pulse-up ratios (over the low mode) of 3 to 5 have been considered for a 10:1 pulse-up in output power. However, this introduces some severe problems in the areas of beam optics and control (especially for PPM focused TWT's) and in TWT circuit design since a number of important TWT parameters are functions of the beam current and effective beam radius.

The required pulse-up in beam current can be significantly reduced, and the associated problems mitigated, if the low mode can represent operation of the TWT well below saturation. This alternative approach is practical only if an extremely efficient (>90 percent) depressed collector for the low mode can be used to insure a reasonable TWT overall efficiency. The problem of developing such a collector, however, is compounded by the fact that the collector operation cannot be optimized for the low mode: Extreme collector depression for the low mode (well below saturation) can produce a disastrous amount of backstreaming to the TWT in the pulsed-up mode and subsequent TWT failure. Therefore, the MDC optimization involves a compromise between the two operating modes.

In order to evaluate the effectiveness of this type of

MDC for a fixed set of operating conditions over a 10:1 pulse-up range, where the high mode represents saturated operation (the most difficult case) and the low mode cw operation well below saturation (8 dB for this TWT), the dual-mode TWT was operated over the range of output powers of 83 to 830 watts. The compromise collector optimizations performed favored the low (cw) mode since the high (pulsed-up) mode often represents a very low duty-cycle application. Data were also taken at intermediate levels of output power using these fixed sets of five-, four-, and three-stage collector operating conditions. The results are shown in table III. It is evident that an effective compromise can be achieved and very high collector efficiencies obtained for the low mode. For this wide range of TWT operating conditions, each additional depressed stage (four versus three and five versus four) produced a significant increase in both the collector and TWT overall efficiencies. A minimum overall efficiency in excess of 20 percent was obtained with the five-stage collector. The collector voltages used (normalized to V_k) were the following:

(1) Five stage – 1.0, 0.97, 0.84, 0.66, and 0.56
(2) Four stage – 1.0, 0.95, 0.76, and 0.56
(3) Three stage – 1.0, 0.94, and 0.55.

In order to evaluate the TWT-MDC performance as a function of frequency for a fixed set of MDC operating conditions, the TWT and four-stage collector were operated at a constant rf output power of about 83 watts over an octave bandwidth for the fixed MDC and refocusing system conditions used to generate the data of table III(b). The results are shown in figure 10(b). It is evident that both the TWT and MDC performances are highly insensitive to the operating frequency as such.

A 10:1 pulse-up in output power was emphasized in these tests. For smaller pulse-up ratios and in particular where the high mode also represents operation below saturation (e.g., ref. 5), significantly higher collector and overall efficiencies should be possible (through individual optimization for each case) than those shown in table III, which emphasized maximum overall efficiency at the 10:1 point.

The collector efficiencies for the dc (unmodulated) beam, for these fixed sets of MDC operating conditions, are also shown in table III. The 92 to 95 percent collector efficiencies are indicative of those obtainable for the application where the dc beam must be "on" at all times and the modulated TWT operated at saturation. For the case where the modulated TWT is operated several decibels below saturation, significantly higher "dc" collector efficiencies could be obtained than are obtained for TWT's operated at or near saturation (see ref. 6).

Dual-mode TWT-MDC performance at saturation. – In order to evaluate the MDC performance when the TWT is pulsed between the high and low modes, at a fixed set of operating conditions, five-, four-, and three-stage collector performance was individually optimized near midband in the low (cw) mode. The TWT-MDC performance in both the high and low modes was then evaluated across an octave bandwidth for the fixed set of MDC and refocusing-system operating conditions.

The results are shown in tables IV to VI for the five-, four-, and three-stage collectors, respectively.

TABLE III. – DUAL-MODE TWT-MDC PERFORMANCE AT AND BELOW SATURATION FOR A FIXED SET OF MDC OPERATING CONDITIONS (9.2 GHz)

(a) Five-stage collector

Mode	Pulse-up ratio, $\frac{P_{rf(\text{high mode})}}{P_{rf(\text{low mode})}}$	Overall efficiency, percent		Collector efficiency, percent
		Without MDC	With MDC	
High	1.0 (saturation)	17.2	42.6	76.6
Low	2.0	11.1	39.8	83.6
	3.0	7.4	35.4	87.1
	4.0	5.5	32.4	89.2
	5.0	4.4	29.2	90.1
	6.0	3.7	27.2	90.9
	7.0	3.1	24.9	91.4
	8.0	2.8	23.1	91.6
	9.0	2.5	21.7	91.9
	10.0	2.2	20.6	92.3
	dc beam	----	----	95.2

(b) Four-stage collector

High	1.0 (saturation)	17.2	41.2	74.7
Low	2.0	11.0	40.9	84.6
	3.0	7.3	36.3	87.9
	4.0	5.5	32.1	89.1
	5.0	4.4	28.7	89.9
	6.0	3.7	25.8	90.1
	7.0	3.1	23.5	90.5
	8.0	2.8	21.7	90.8
	9.0	2.5	19.8	90.8
	10.0	2.2	18.8	91.2
	dc beam	----	----	93.8

(c) Three-stage collector

High	1.0 (saturation)	17.0	40.9	74.8
Low	2.0	11.1	38.0	82.0
	3.0	7.3	31.7	84.6
	4.0	5.5	27.4	85.9
	5.0	4.4	23.8	86.4
	6.0	3.7	21.2	86.8
	7.0	3.2	19.0	87.2
	8.0	2.8	17.4	87.6
	9.0	2.5	15.9	87.6
	10.0	2.2	14.4	87.5
	dc beam	----	----	92.5

TABLE IV. – DUAL-MODE TWT AND FIVE-STAGE COLLECTOR PERFORMANCE ACROSS AN OCTAVE BANDWIDTH AND AT SATURATION FOR A FIXED SET OF MDC OPERATING CONDITIONS

(a) Low mode

Frequency GHz	Overall efficiency[a] percent		Collector efficiency, percent
	Without MDC	With MDC	
4.8	8.6	36.7	86.4
5.2	10.2	41.2	86.2
5.6	10.8	42.2	86.5
6.0	11.5	44.7	87.1
6.4	13.6	49.5	86.8
6.8	13.0	47.7	86.9
7.2	12.8	47.3	87.1
7.6	12.5	45.7	86.3
8.0	13.0	46.3	85.8
8.4	13.2	46.8	86.0
8.8	13.3	47.9	86.7
9.2	13.3	48.4	86.9
9.6	12.3	46.8	87.5

(b) High mode

4.8	10.5	36.9	84.2
5.2	12.2	41.4	84.1
5.6	12.3	41.6	84.6
6.0	12.1	41.5	85.7
6.4	15.4	49.6	85.3
6.8	14.5	46.6	84.7
7.2	14.5	46.1	85.4
7.6	14.9	47.7	85.8
8.0	16.0	49.6	85.5
8.4	16.4	50.8	86.0
8.8	17.0	51.6	86.0
9.2	17.2	51.9	85.8
9.6	16.6	50.1	85.1

[a]Based on the total rf power generated.

TABLE V. – DUAL-MODE TWT AND FOUR-STAGE COLLECTOR PERFORMANCE ACROSS AN OCTAVE BAND-WIDTH AND AT SATURATION FOR A FIXED SET OF MDC OPERATING CONDITIONS

(a) Low mode

Frequency GHz	Overall efficiency,[a] percent		Collector efficiency, percent
	Without MDC	With MDC	
4.8	8.7	35.6	85.4
5.2	10.4	41.0	85.7
5.6	10.9	41.1	85.3
6.0	12.0	43.9	85.7
6.4	13.5	47.3	85.4
6.8	13.1	45.1	84.8
7.2	12.8	44.4	85.1
7.6	12.6	44.3	85.1
8.0	13.0	43.9	83.9
8.4	13.2	44.1	83.8
8.8	13.3	44.9	84.6
9.2	13.5	46.5	85.2
9.6	12.6	45.9	86.3

(b) High mode

4.8	10.5	35.8	83.2
5.2	12.0	39.8	83.2
5.6	12.4	39.9	82.9
6.0	12.5	39.8	83.4
6.4	15.2	45.6	82.2
6.8	14.6	43.8	82.0
7.2	14.6	42.8	82.1
7.6	15.1	44.1	82.1
8.0	16.2	46.1	82.1
8.4	16.6	47.4	82.9
8.8	16.9	47.6	82.4
9.2	17.3	48.5	82.6
9.6	16.7	47.0	82.3

[a]Based on the total rf power generated

TABLE VI. – DUAL MODE TWT AND THREE-STAGE COLLECTOR PERFORMANCE ACROSS AN OCTAVE BANDWIDTH AT SATURATION FOR A FIXED SET OF MDC OPERATING CONDITIONS

(a) Low mode

Frequency GHz	Overall efficiency,[a] percent		Collector efficiency, percent
	Without MDC	With MDC	
4.8	8.7	32.4	82.7
5.2	10.4	36.9	82.4
5.6	10.9	36.7	81.8
6.0	11.7	38.9	82.0
6.4	13.5	42.4	81.4
6.8	13.0	41.0	81.5
7.2	12.8	40.5	81.7
7.6	12.6	39.9	81.4
8.0	12.9	40.1	80.9
8.4	13.2	41.1	81.3
8.8	13.3	41.5	81.5
9.2	13.4	42.3	81.9
9.6	12.5	41.5	83.0

(b) High mode

4.8	10.7	34.6	81.5
5.2	12.0	38.2	81.7
5.6	12.4	37.6	80.7
6.0	12.5	37.9	81.3
6.4	15.1	42.3	79.3
6.8	14.6	41.0	79.3
7.2	14.6	40.5	79.6
7.6	15.0	41.6	79.9
8.0	16.0	43.3	79.6
8.4	16.6	44.1	79.5
8.8	17.0	44.4	79.0
9.2	17.2	44.7	78.9
9.6	16.6	43.9	79.2

[a]Based on the total rf power generated.

A very significant improvement in the TWT overall efficiency was obtained with each of the MDC's. With the five-stage collector the average overall efficiency (based on P_{rf}) across the octave bandwidth was improved from 12.2 percent (no MDC) to 45.5 percent (with MDC) in the low mode and from 14.6 percent to 46.5 percent in the high mode.

The TWT and collector performance for the low and high modes is compared in figure 11. The collector efficiencies are somewhat higher in the low mode, partly because the collector performance was optimized in the low mode to minimize the prime power needed for cw operation. When optimized for the high mode significantly smaller differences in collector performance for the two modes can be expected (ref. 6). The overall efficiencies in the two modes are quite comparable; the lower electronic efficiencies in the low mode are offset by the higher collector efficiencies and smaller relative fixed TWT losses (see, fig. 6) of the low mode.

The TWT overall and collector efficiencies obtained with the three MDC's are compared in figures 12 and 13, respectively. A significant improvement in both overall and collector efficiencies was obtained from each additional stage (four versus three and five versus four). However, with a fully optimized MDC geometric design for each MDC (number of stages), smaller differences in performance might be ex-

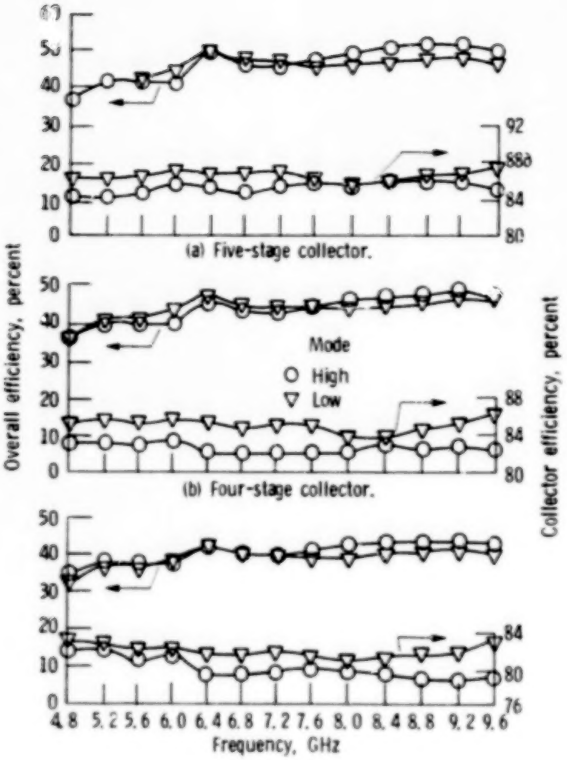

Figure 11. - TWT overall and MDC efficiencies versus frequency at saturation.

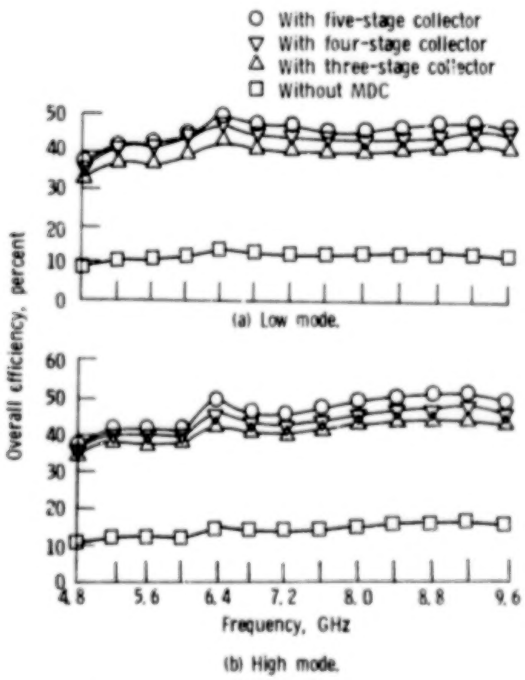

Figure 12. - Overall efficiency versus frequency at saturation.

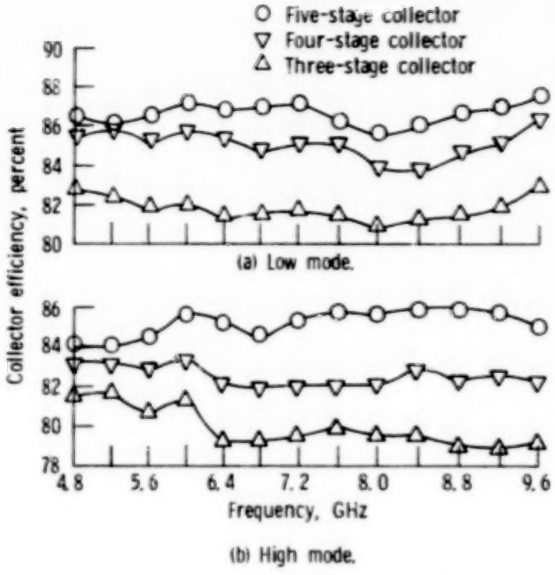

Figure 13. - Collector efficiency versus frequency at saturation.

pected. The performance of each collector was found to be relatively constant across the octave bandwidth in spite of substantial changes in rf output power.

The overall efficiencies reported in this section have been based on the total rf power generated P_{rf}, these being indicative of efficiencies obtainable with excellent harmonic suppression (normally used with this type of TWT). To obtain efficiencies based on P_{fund}, the overall efficiencies (both with and without the MDC) in the range of operating frequencies of 4.8 to 5.6 gigahertz should be multiplied by the following approximate factors (see figs. 6 and 7):

Frequency, Ghz	P_{fund}/P_{rf}	
	Low mode	High mode
4.8	0.7	0.62
5.2	.86	.72
5.6	.99	.87

The collector voltages (normalized to V_k) used were

(1) Five stage – 1.0, 0.95, 0.78, 0.61, and 0.56
(2) Four stage – 1.0, 0.95, 0.83, and 0.56
(3) Three stage – 1.0, 0.90, and 0.55.

Collector voltage variations. – The degree of voltage regulation required for the collector power supply for operation of the TWT in the linear region

was evaluated by determining the performances of the TWT and collector as functions of collector voltages. Starting with the fixed set of refocusing system and MDC operating conditions used to generate the data of table III(b), all the collector voltages (except the electrode at cathode potential) were varied by fixed ratios above and below the nominal values. A constant rf output power of nominally 85 watts was maintained.

The results are shown in figure 14. A 1-percentage-point reduction in the overall TWT efficiency resulted from a ±2.5 percent collector voltage variation. Similar results were obtained for MDC performance optimized for operation of the TWT in the linear range.

Collector efficiency as a function of collector voltages for operation of the TWT at saturation are reported in reference 8.

Effectiveness of carbon black coating for suppression of secondary electrons. – In order to get a measure of the effectiveness of the carbon-black coating (soot) used for the suppression of secondary electrons, representative tests initially made with a coated MDC were repeated with uncoated copper electrodes. The uncoated tests were optimized for the new condition rather than using the collector voltages and focusing coil currents obtained with the optimized coated tests. This permitted a comparison of the best performances possible for coated and uncoated MDC's that are otherwise physically identical.

The collector efficiency losses without the carbon black coating were substantial in all cases. For operation of the TWT in the linear range, the loss in collector efficiency had a strong correlation with the rf output power, varying from 2½ percentage points for the dc beam to about 4½ percentage points at the upper end of the linear range. For operation of the TWT at saturation in the low mode across the octave bandwidth, the average loss in collector efficiency was approximately 4½ percentage points.

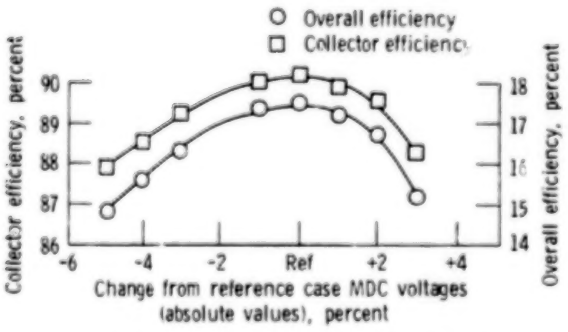

Figure 14. - Variation in MDC and overall efficiencies as function of small changes in MDC voltages. Reference case: Same conditions as used to generate data of table III (b); rf output power nominally 85 watts.

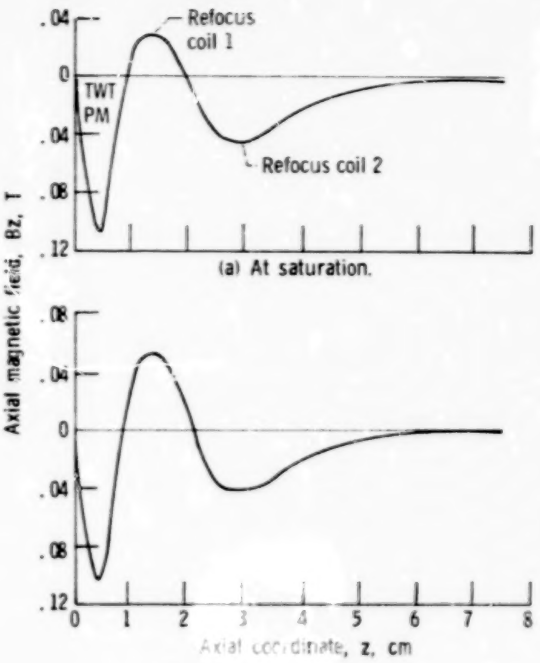

Figure 15. - Typical refocusing profiles for operation of the TWT.

The limitations regarding tests with this particular TWT-MDC arrangement should be noted again. This MDC with coating was the best experimental optimization to be developed for an octave-bandwidth (4.8 to 9.6 GHz) single-mode TWT (ref. 2). The MDC is not optimum for the dual-mode TWT used in these tests. As such, efficiency differences are most likely exaggerated because of excessive secondary emission and resultant backstreaming when using an uncoated, unoptimized MDC.

Role of spent-beam refocusing in the optimization of MDC performance. – The benefits of spent-beam refocusing have been described in references 3 and 4. In the experiments described herein the variable spent-beam refocusing system played a key role in obtaining very high MDC efficiencies for each of the wide range of TWT applications investigated. Each application produces a spent electron beam that is characterized by the individual electron velocities ($\vec{v}$ (r,z,θ)) and positions (r,z,θ) and determines the optimum set of collector voltages for a given number of stages. These spent beams differ vastly (in radii, energies, and electron angles) for the range of TWT applications considered here. Injecting these various beams into a collector of fixed geometry (and adjusted to the optimum set of voltages) can severely compromise the collector efficiency in some cases due to a combination of harmful lens effects (see e.g., ref. 10) and improper collector electrode aperture sizes. (The reduced MDC efficiencies for the

high mode in the compromise optimization are examples of this.) The refocusing system was found to be very effective (for a given application) in "adapting" the various spent-beam injection conditions (electron radii and angles at the collector input) to the MDC geometric design used. This is an indirect benefit of spent-beam refocusing: it is much easier to change the refocusing system (exterior to the vacuum envelope of the TWT) than to modify the MDC geometry.

Typical refocusing field profiles for the extreme cases of saturated operation of the TWT and of operation in the low end of the linear range are shown in figure 15.

Concluding Remarks

An axisymmetric depressed collector of fixed geometric design was optimized and evaluated over a wide range of TWT and MDC operating conditions. The combination of refocusing system and MDC proved to be highly adaptable to the wide range of TWT applications considered. Each additional depressed stage (four versus three and five versus four) produced a significant increase in the collector and TWT overall efficiencies for each of the applications covered.

The very high five-stage collector efficiencies achieved in combination with the relatively low fixed losses of this TWT sample enabled the demonstration of

1. Overall efficiencies of up to 34 percent for operation of the TWT in the linear, low-distortion range.

2. A minimum overall efficiency of 20 percent for operation of the dual-mode TWT over a 10:1 range in output power.

3. Overall efficiencies in the range of 40 to 50 percent for both the high and low modes at saturation over most of the octave bandwidth.

The variable spent beam refocusing system played a key role in obtaining these results with a single MDC of fixed geometric design.

For operation of the dual-mode TWT over a 10:1 range in output power, the compromise optimization resulted in less than a percentage-point loss in collector efficiency for the low mode. The loss in performance for the pulse-up mode, however, was substantial. A modification of the MDC geometric design is required to minimize this loss in collector performance for the cases of compromise optimization.

For operation of the TWT in the linear range, with collector efficiencies in excess of 90 percent, beam interception losses can become a substantial fraction of the total losses in the TWT-MDC system and exert a strong effect on the TWT overall efficiency. Therefore, minimizing these losses becomes very important.

Lewis Research Center,
National Aeronautics and Space Administration,
Cleveland, Ohio, October 5, 1979,
506-20.

References

1. Kosmahl, Henry G.: A Novel, Axisymmetric, Electrostatic Collector for Linear Beam Microwave Tubes. NASA TN D-6093, 1971.
2. Kosmahl, Henry G.; and Ramins, Peter: Small-Size 81- to 83.5-Percent Efficient 2- and 4-Stage Depressed Collectors for Octave-Bandwidth High-Performance TWT's. IEEE Trans. Electron Devices, vol. ED-24, no. 1, Jan. 1977, pp. 36-44.
3. Kosmahl, Henry G.: An Electron Beam Controller. U.S. Patent 3, 764, 850, Oct. 1973.
4. Stankiewicz, N.: Analysis of Spent Beam Refocusing to Achieve Optimum Collector Efficiency. IEEE Trans. Electron Devices, vol. ED-24, no. 1, Jan. 1977, pp. 32-36.
5. Stankiewicz, N.; and Anzic, G.: TWT Design Requirements for 30/20 GHz Digital Communications Satellite. NASA TM-79119, 1979.
6. Ramins, P.; and Fox, T. A.: Efficiency Enhancement of Dual-Mode TWT's at Saturation and in the Linear Range by the Use of Spent Beam Refocusing and Multistage Depressed Collectors. NASA TP-1486, 1979.
7. Kosmahl, Henry G.: Comments on Measuring the Overall and Depressed Collector Efficiency in TWT's and Klystron Amplifiers. IEEE Trans. Electron Devices, vol. ED-26, no. 2, Feb. 1979.
8. Ramins, P.; and Fox, T. A.: Efficiency Enhancement of Octave-Bandwidth Traveling Wave Tubes by Use of Multistage Depressed Collectors. NASA TP-1416, 1979.
9. Gilmour, A. S., Jr.: Bakeable Ultra-High Vacuum Gate Valve for Microwave Tube Experimentation. J. Vac. Sci. Technol., vol. 13, no. 6, Nov.-Dec. 1976, pp. 1199-1201.
10. Dayton, J. A., Jr.; et al.: Analytical Prediction with Multidimensional Computer Programs and Experimental Verification of the Performance, at a Variety of Operating Conditions, of Two Traveling Wave Tubes with Depressed Collectors. NASA TP-1449, 1979.

1. Report No. NASA TP-1670	2. Government Accession No.	3. Recipient's Catalog No.
4. Title and Subtitle MULTISTAGE DEPRESSED COLLECTOR WITH EFFICIENCY OF 90 TO 94 PERCENT FOR OPERATION OF A DUAL-MODE TRAVELING-WAVE TUBE IN THE LINEAR REGION		5. Report Date April 1980 6. Performing Organization Code
7. Author(s) Peter Ramins and Thomas A. Fox		8. Performing Organization Report No. E-9975 10. Work Unit No. 506-20
9. Performing Organization Name and Address National Aeronautics and Space Administration Lewis Research Center Cleveland, Ohio 44135		11. Contract or Grant No.
12. Sponsoring Agency Name and Address National Aeronautics and Space Administration Washington, D.C. 20546		13. Type of Report and Period Covered Technical Paper 14. Sponsoring Agency Code
15. Supplementary Notes		

16. Abstract

An axisymmetric, multistage, depressed collector of fixed geometric design was evaluated in conjunction with an octave-bandwidth, dual-mode traveling-wave tube (TWT). The TWT was operated over a wide range of conditions to simulate different applications. The collector performance was optimized (within the constraint of fixed geometric design) over the range of TWT operating conditions covered. For operation of the TWT in the linear, low-distortion range, 90 percent and greater collector efficiencies were obtained leading to TWT overall efficiencies of 20 to 35 percent, as compared with 2 to 5 percent with an undepressed collector. With collectors of this efficiency and minimized beam-interception losses, it becomes practical to design dual-mode TWT's such that the low mode can represent operation well below saturation. Consequently, the required pulse-up in beam current can be reduced or eliminated, and this mitigates beam control and dual-mode TWT circuit design problems. For operation of the dual-mode TWT at saturation, average collector efficiencies in excess of 85 percent were obtained for both the low and high modes across an octave bandwidth, leading to a three- to fourfold increase in the TWT overall efficiency.

17. Key Words (Suggested by Author(s))	18. Distribution Statement
Traveling wave tubes Multi-stage depressed collectors	Unclassified - unlimited STAR Category 33

19. Security Classif. (of this report)	20. Security Classif. (of this page)	21. No. of Pages	22. Price*
Unclassified	Unclassified	15	A02

*For sale by the National Technical Information Service, Springfield, Virginia 22161

NASA-Langley, 1980